Defining Folding and Unfolding Reactions of Apocytochrome b_5 Using Equilibrium and Kinetic Fluorescence Measurements†

Susan Manyusa and David Whitford*

Structural Biochemistry, Molecular & Cellular Biology, Division of Biomedical Sciences, Queen Mary & Westfield College, London E1 4NS, U.K.

Received March 9, 1999; Revised Manuscript Received April 20, 1999

ABSTRACT: The refolding and unfolding kinetics of a soluble domain of apocytochrome b_5 extending from residue 1 to 104 have been characterized using stopped flow and equilibrium-based fluorescence methods. The isolated apoprotein unfolds reversibly in the presence of GuHCl. From cooperative unfolding curves, the conformational stability (ΔG_{uw}), in the absence of denaturant, is estimated to be 11.6 ± 1.5 kJ mol^{-1} at 10 °C. The stability of apocytochrome b_5 is lower than that of the corresponding form of the holoprotein ($\Delta G \sim 25$ kJ mol^{-1}) and exhibits a transition midpoint at 1.6 M GuHCl. Kinetic studies support the concept of a two-state model with both unfolding and refolding rates showing an exponential dependence on denaturant concentration with no evidence of the formation of transient intermediates in either limb of the chevron plot. Apocytochrome b_5 is therefore an example of a protein in which both kinetics and equilibria associated with folding are described by a two-state model. The values of m_{ku} and m_{kf} obtained from kinetic analysis are an indication of a transition state (m_{ku}/m_{eq} of 0.29) that resembles the native form by retaining similar solvent accessibility and many of the noncovalent interactions found in the apoprotein. The changes in heat capacity support a transition state that resembles the apoprotein with a value for ΔC_{pf} of −3.6 kJ mol^{-1} K^{-1} estimated for the refolding reaction. From these measurements, a model of refolding that involves the rapid nucleation of hydrophobic residues around Trp26 is suggested as a major event in the formation of the native apoprotein.

The mechanism by which proteins assemble into specific three-dimensional folds remains a major experimental and theoretical problem in structural biology. In this area, kinetic studies with small soluble proteins such as lysozyme, CI2, α-lactalbumin, myoglobin, and barnase have provided a wealth of experimental data. These studies have shown that solvent exclusion, formation of secondary structure, hydrophobic collapse, multiple transition states, and intermediates can be recognized as integral reactions within the overall folding process (*1*−*3*). Proteins containing a cofactor present a more complicated folding system since integration of the prosthetic group is a necessary prerequisite in the formation of the native, functional, state. One approach that overcomes these problems is studying the apo form of these proteins in the expectation that they will provide a kinetically simpler system.

The thermodynamic and kinetic parameters associated with the folding of apocytochrome b_5 have not been described to date, and the absence of highly defined structures comparable to the holoprotein hinders mechanistic studies. In the native state, cytochrome b_5 contains both α-helices and β-strands with helices 2−5 surrounding the heme and creating part of a hydrophobic pocket with an antiparallel β-strand providing the base to this assembly (*4*−*6*). This mixed α/β structure coupled with bis-histidine ligation of the heme provides a stable framework (*7*−*9*). The conformational stability and overall structure of cytochrome b_5 are strongly influenced by the heme group. Differential scanning calorimetry has estimated values for the conformational stability (ΔG_{298}) of the holo and apo forms of 25 and 7 kJ mol^{-1}, respectively (*9*). The decline in stability accompanies a loss of helical structure, and CD spectroscopy has shown that apo- and holocytochrome b_5 possess different far- and near-UV spectra (*10*). Although the apoprotein retains both secondary and tertiary structure, the helical content decreases from 38 to 21% (*11*, *12*), and this is supported by NMR studies (*13*). Second-derivative absorbance spectroscopy indicates that increased solvent exposure occurs for Phe residues in the apoprotein when compared with holocytochrome b_5, although the single Trp and four Tyr residues remain in similar environments. Additionally, spectroscopic studies have shown that removal of the heme group does not change the intrinsically low fluorescence associated with the solitary tryptophan residue. The soluble domain of apocytochrome b_5 retains properties similar to those seen in the holoprotein (*10*). Determination of the crystallographic structure of holocytochrome b_5 suggested that a close interaction between the aromatic rings of Trp26 and His19 accounted for the low fluorescence (*4*) and pointed to the retention of this interaction in the apoprotein after heme extraction.

† This work was supported by project grants from the Wellcome Trust and BBSRC. The BBSRC is thanked for studentship support to S.M.

* To whom correspondence should be addressed: Structural Biochemistry, Molecular & Cellular Biology, Biomedical Sciences, Queen Mary & Westfield College, London E1 4NS, U.K. E-mail: D.Whitford@qmw.ac.uk. Telephone: 44-171-9826349. Fax: 44-181-9830531.

10.1021/bi990550d CCC: $18.00
Published on Web 07/01/1999

In contrast to the crystal and solution structures that are available for rat and bovine cytochrome b_5, the structure of the corresponding apoprotein is less well defined. Apocytochrome b_5 is usually isolated after extraction of the heme group using organic solvents, and this form of the protein has been studied using NMR spectroscopy (*13*−*15*). Two-dimensional NMR spectroscopy of ^{15}N-enriched apocytochrome b_5 indicates a partially folded structure with β-strands from residue 24 to 29, 32 to 37, and 56 to 58 remaining largely intact along with three short α-helices. However, three of the four helices that form much of the heme binding pocket are either partially formed or undetected (*13*). However, a significant aspect of the solution structure determined for the apoprotein was the presence of a stable hydrophobic core around Trp26. This core is believed to be capable of rapid, independent assembly (*15*). Cytochrome b_5 is therefore envisaged as two modules in which core 2, centered around Trp26, acts as a structural unit capable of organizing the potential heme binding site (*13*). This structure may have some relevance to the folding mechanism in vivo since it has been demonstrated that protein synthesis yields substantial amounts of the apo form prior to the insertion of heme (*16*) and that heme synthesis occurs within the mitochondrion (*17*).

Considerable insight into the folding of apoproteins has been obtained using apomyoglobin as a model system (*18*). Unlike cytochrome b_5, the holoprotein is totally α-helical and possesses a five-coordinate iron center. Removal of the heme leaves a folded protein with extensive (30%) helical structure around pH 7.0, while lowering the solution pH to mildly acidic conditions yields an intermediate state termed the molten globule form (*19*). From amide exchange experiments, a subdomain consisting of helices A, G, and H has been identified in the acid form of apomyoglobin, and this has been equated with the early folding intermediate detected in kinetic studies (*20*). In comparison with apomyoglobin, the folding pathway of apocytochrome b_5 is poorly described. The existence of molten globule states or kinetic intermediates has not yet been confirmed, and this has hindered the pursuit of knowledge of the folding pathway of cytochrome b_5. Moore and Lecomte (*15*) have shown that the refolding of urea-denatured apocytochrome b_5 exhibits triphasic kinetics with observed rates of 70, 2, and 0.06 s^{-1}, although the origins of these three phases and, for example, their dependence on denaturant concentration and temperature were not further investigated. The absence of detailed kinetic- and equilibrium-based data for the unfolding and refolding pathways of apocytochrome b_5 has led to a detailed analysis of this system. More importantly, the stability and folding of the apocytochrome b_5 represents a necessary prerequisite for any study of holoproteins.

EXPERIMENTAL PROCEDURES

Protein Purification and Reagents. All reagents were of Analar grade, and solutions were filtered through 0.45 μm filters prior to use. Ultrapure GuHCl[1] was purchased from either Calbiochem or Melford, UK, and solutions were made gravimetrically with further verification using refractive index measurements (*21*). The apoprotein concentration was determined using the absorbance at 280 nm for which an extinction coefficient of 10.6 mM^{-1} cm^{-1} has been determined previously (*13*, *22*). The Ala1−Ser104 variant of bovine cytochrome b_5 was expressed and purified as described previously (*8*). The apoprotein was made from the purified holoprotein using an adaptation of the method of Teale (*23*). The heme was removed by dropwise addition of 0.1 M HCl to a cytochrome b_5 solution (final concentration of 1 mM) at 4 °C, until the pH was between 2.3 and 3.0. An equal volume of butanone was added immediately, and the mixture was left on ice until two immiscible phases formed. The upper colored phase was discarded, while the lower layer was collected. Residual heme was removed by re-extraction of the aqueous phase with another equal volume of butanone. The resulting pale yellow solution was dialyzed overnight against distilled water at 4 °C. The dialyzed material was briefly centrifuged to remove precipitated material, lyophilized in small (50−100 μL) aliqouts, and stored at −20 °C until it was used further. Samples of apocytochrome b_5 used in stopped flow and equilibrium experiments were added to the appropriate buffer immediately prior to use.

Equilibrium Measurements of Apoprotein Unfolding. Apoprotein unfolding was assessed by measuring the fluorescence of Trp26 at different concentrations of GuHCl using an SLM-Aminco 8100 spectrofluorimeter. An excitation wavelength of 280 nm was routinely used with a monochromator slit width of 4 nm. All emission spectra were scanned between 300 and 400 nm at a rate of 1 nm s^{-1} using two monochromators adjusted to a slit width of 4 nm. For each GuHCl concentration, a suitable blank solution was subtracted from the same solution containing 1−2 μM protein. The fluorescence intensity at 349 nm in each spectrum was measured at a range of denaturant concentrations and used to estimate the conformational stability in the absence of denaturant (ΔG_{uw}) and its dependence on denaturant concentration (m_{eq}) via the combination of eqs 1 and 2

$$F = [F_N + F_U \exp(-\Delta G_u/RT)]/[1 + \exp(-\Delta G_u/RT)] \quad (1)$$

$$\Delta G_u = \Delta G_{uw} - m_{eq}[\text{GuHCl}] \quad (2)$$

Kinetic Measurements of Apoprotein Folding. All kinetic measurements of protein refolding or unfolding were performed using an Applied Photophysics stopped flow SX18MV system. In the absence of the heme group, the fluorescence emission above 320 nm was used to study these processes. Fluorescence data sets were recorded using a 2 mm path length and by measuring the intensity at 90° to the excitation wavelength (280 nm) after passing through a 320 nm cutoff filter. Data were collected at time intervals ranging from 10 ms to 1000 s using between 1000 and 4000 data points. The data recorded at each denaturant concentration are the average of five successive traces, and all traces were fitted to monoexponential relaxation curves using software supplied by Applied Photophysics Ltd.

All folding and unfolding reactions were performed at 10 °C. Unfolding reactions involved mixing the apoprotein with

[1] Abbreviations: GuHCl, guanidine hydrochloride; k_{obs}, observed rate constant; k_{uw} and k_{fw}, first-order rate constant for protein unfolding and folding, respectively, extrapolated to zero denaturant concentration; Ala1−Ser104, soluble domain of cytochrome b_5 extending from residue 1 to 104; m_{eq}, dependence of the free energy of unfolding on GuHCl concentration; m_{ku} and m_{kf}, dependence of the rate of protein folding and unfolding, respectively, on GuHCl concentration; ΔC_{pu}, heat capacity change between folded and transition states.

a 10-fold excess of denaturant to yield final concentrations between 1.6 and 5 M. The kinetics associated with refolding involved mixing 1 volume of unfolded protein with a 6−10-fold excess of 30 mM MOPS (pH 7.0). The unfolded protein had previously been equilibrated in concentrations of GuHCl between 1.6 and 4.5 M for 1 h. The final denaturant concentration ranged from 0.2 to 1.4 M GuHCl. In all of the experiments described here, the final protein concentration was 1 μM.

The kinetic data were analyzed by plotting the unfolding and refolding rates as a function of denaturant concentration in semilogarithmic plots according to eqs 3 and 4.

$$\ln k_u = \ln k_{uw} + m_u[\text{GuHCl}] \quad (3)$$

$$\ln k_f = \ln k_{fw} - m_f[\text{GuHCl}] \quad (4)$$

Combining eqs 3 and 4 allows the observed rate of folding at any concentration of GuHCl to be obtained and was used to estimate the best fit of experimental data. In eqs 3 and 4, $m_{ku} = RTm_u$ and $m_{kf} = RTm_f$.

Temperature Dependency of Protein Folding Reactions. In view of the sensitivity of apocytochrome b_5 to temperatures above 25 °C, a limited temperature range was used to study refolding and unfolding. The unfolding rate was determined at denaturant concentrations between 1.6 and 4.5 M, and for each data set, the rate of reaction in the absence of denaturant (k_{uw}) was estimated from semilogarithmic plots. The values determined for k_{uw} at each temperature were used to calculate the activation parameters for protein unfolding via Eyring plots using the equation shown below:

$$\ln(k_w/T) = \ln(k_b/h) + \Delta S^{\ddagger}/R - \Delta H^{\ddagger}/RT \quad (5)$$

derived from transition state theory (*24*) where k_w is the rate at zero denaturant concentration, $\Delta S^{\ddagger}$ is the activation entropy associated with protein unfolding and/or refolding, $\Delta H^{\ddagger}$ is the activation enthalpy of protein unfolding and/or refolding, and k_b and h are Boltzmann's and Planck's constants, respectively. For all data sets, the temperature was regulated to within ±0.1 °C through the use of a microprocessor-controlled Neslab RTE-111 thermocirculator. For protein refolding, significant curvature was noted in the Eyring plot and eq 6 was used to estimate the magnitude of ΔC_p (*25*).

$$\ln(k_f/T) = \ln(k_b/h) + \Delta S_f(T_0)/R - \Delta H_f(T_0)/RT - \Delta C_p(T - T_0)/RT + \Delta C_p/R \ln(T/T_0) \quad (6)$$

RESULTS

Equilibrium Unfolding Studies of Apocytochrome b_5. Equilibrium measurements of the unfolding of apocytochrome b_5 in GuHCl have not been extensively described. Under solution conditions that promote the folded conformation of apocytochrome b_5, the fluorescence spectrum exhibits a maximum at 335 nm which progressively increases in intensity with higher denaturant concentrations to yield spectra with maxima at 349 nm. Representative normalized data are shown in Figure 1 for the emission spectra of folded and unfolded apocytochrome b_5 at denaturant concentrations of 0.2, 1.4, and 2.6 M GuHCl. The spectra of the unfolded protein exhibit significant asymmetry with a pronounced shoulder around 380 nm. The origin of this shoulder is unclear but may reflect a series of differing microenvironments for the Trp residue in the unfolded conformation and has been noted in other systems (*26*). From spectra recorded at a range of denaturant concentrations between 0 and 3.4 M, the intensity of the fluorescence at 349 nm was used to measure the extent of protein unfolding. The results shown in Figure 2 reveal that apocytochrome b_5 unfolds in a single cooperative curve in which there is no detectable intermediate. The midpoint for the transition occurs at a concentration of 1.6 M GuHCl, and the data are fitted on the assumption that the unfolding equilibria is described by a two-state system in which only the native (N) and unfolded (U) states are significantly populated. From the data of Figure 2, values of m_{eq} and ΔG_{uw} for the unfolding of apocytochrome b_5 are obtained. This approach yielded an average value of 11.6 ± 1.5 kJ mol^{-1} for the stability of the apoprotein in the absence of denaturant (ΔG_{uw}) and a value for m_{eq} of 7874 ± 181 J mol^{-1} M^{-1}. The value of m_{eq} is a constant proportional to the increase in the level of solvent exposure of the protein during the unfolding reaction.

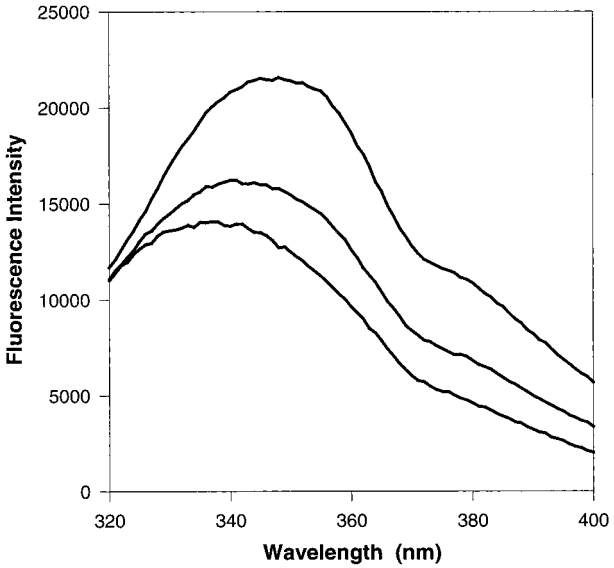

FIGURE 1: Emission spectra between 320 and 400 nm for folded and unfolded forms of bovine microsomal apocytochrome b_5. The spectra were recorded between 320 and 400 nm with an excitation wavelength of 280 nm (emission and excitation slit widths of 4 nm) at a protein concentration of 1.5 μM in 30 mM MOPS (pH 7.0). The spectra were corrected for differential photomultiplier response and any background fluorescence of the buffer by subtraction. The spectra were recorded at the following denaturant concentrations: 0.2, 1.4, and 2.4 M GuHCl.

Kinetic Studies of Refolding and Unfolding Reactions. From the data shown in Figure 2, solution conditions promoting folding and unfolding in apocytochrome b_5 were defined for subsequent kinetic measurements. The apoprotein remains largely folded below 0.6 M GuHCl, while above 2.0 M, the protein assumes a largely disordered state. The kinetics of apoprotein unfolding can be followed using the time-dependent increase in Trp fluorescence above 320 nm. The increase in fluorescence in the presence of 4 M GuHCl is shown in Figure 3 and follows a single-exponential process with the reaction being complete within approximately 500 ms. The monoexponential process is emphasized in the plot of the residuals versus time. Consequently, all of the data acquired in this aspect of the current study were modeled by fitting to single-exponential processes. Repeating these

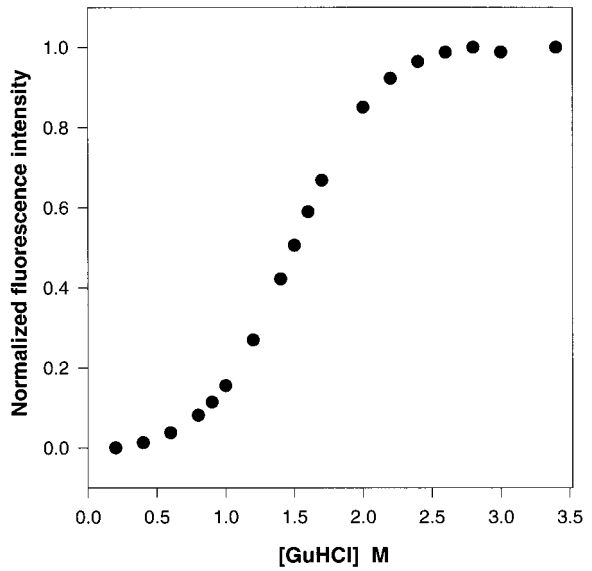

FIGURE 2: Denaturation curve for apocytochrome b_5 determined from changes in Trp fluorescence. The spectrum of apocytochrome b_5 was measured in varying concentrations of denaturant and corrected by subtraction of the background as described in Experimental Procedures. The fluorescence intensity at 349 nm was plotted against denaturant concentration. The data were fitted directly to eq 1 and used to estimate the stability of the apoprotein at zero denaturant concentration. The data were obtained at a protein concentration of 1 μM. No significant variation in the transition midpoint was seen at concentrations of apoprotein between 0.5 and 5 μM.

measurements over a range of denaturant concentrations between 1.6 and 4.5 M allows the intrinsic unfolding rate in the absence of denaturant to be estimated. Semilogarithmic plots of k_u versus denaturant concentration are linear over the complete range of unfolding conditions and when fitted to eq 5 lead to a value for the unfolding rate at 0 M GuHCl (k_{uw}) of 0.24 s^{-1}. The value for m_{ku} of 2420 $\pm$ 420 J mol^{-1} M^{-1} is significantly lower than the equilibrium value (7874 J mol^{-1} M^{-1}) observed for unfolding of the apoprotein and suggests that the transition state for unfolding exhibits solvent accessibility and noncovalent interactions more closely allied to the initial apoprotein. The ratio m_{ku}/m_{eq} is 0.29 and indicates the position of the transition state along the reaction coordinate between unfolded and folded forms of the protein.

The refolding process followed from the fluorescence intensity above 320 nm exhibits a single-exponential decay, and there is no evidence of additional minor phases. For protein refolding, these reactions were continued for up to 100 s with no evidence of significant additional processes such as those seen with proline isomerization (Figure 3). Again the residuals plot clearly demonstrates a satisfactory fit to a monophasic process. By measuring the rate as a function of denaturant concentration, we observed a linear dependence throughout the concentration range (0−1.4 M). In Figure 4, these data are combined to produce a classical chevron plot. The transition midpoint is observed around 1.6 M and agrees closely with that estimated from the equilibrium fluorescence data. Both limbs exhibit a linear dependency on denaturant concentration, and there is little evidence of curvature in these semilogarithmic plots, suggesting that intermediates do not accumulate before the rate-determining steps. From data such as that shown in Figure 4, the rate of refolding at zero denaturant concentration is estimated to be 19.5 s^{-1} while a value for m_{kf} of 5589 $\pm$ 552 J mol^{-1} M^{-1} is obtained. The absence of deviations from linearity in the semilogarithmic plot of the rates of refolding and unfolding versus denaturant concentration suggests that the apo form of cytochrome b_5 behaves as a simple two-state system. In this context, a shorter form of cytochrome b_5 containing the first 90 residues exhibits similar folding kinetics (S. Manyusa and D. Whitford, unpublished results).

Temperature Dependency of Apoprotein Folding. Further insight into the energetics of protein folding and unfolding can be obtained from an analysis of the temperature dependence of each process. The temperature dependency for the unfolding of apocytochrome b_5 was determined at six different temperatures from 8 to 25 °C and at seven different GuHCl concentrations from 1.6 to 4.5 M. Higher temperatures are precluded as a result of the onset of slow thermal denaturation of apocytochrome b_5 above 25 °C (S. Manyusa and D. Whitford unpublished observations, 1998). At each temperature, the linear plots were extrapolated to zero denaturant concentration, and these values are used in the Eyring analysis shown in Figure 5A. The unfolding data reveal a linear plot, with no evidence of curvature, over a temperature range of 17 K. Such plots are generally taken to imply that ΔC_{pu}, the change in heat capacity between the native and transition states, is small ($\Delta C_{pu} \sim 0$). From Figure 5A, the activation enthalpy and entropy for unfolding were determined to be 119.9 $\pm$ 8.45 kJ mol^{-1} and 165.8 $\pm$ 29 J mol^{-1} K^{-1}, respectively (Table 2). If it is assumed that ΔH_u and ΔS_u are independent of temperature, the activation free energy of unfolding is estimated to be 70.5 kJ mol^{-1} at 25 °C.

The temperature dependence of protein refolding was also determined over a similar range. The data shown in the Eyring plot in Figure 5B show significant curvature and deviate from linearity especially when compared with the unfolding data. This suggests that during refolding the heat capacity changes significantly between the unfolded and transition states. We have estimated the magnitude of ΔC_{pf}, the heat capacity change between unfolded and transition states, from the curvature of the data in Figure 5B using eq 6. These activation parameters are summarized in Table 1 using a reference temperature of 25 °C, and the solid line in Figure 5B reflects a value of −3.6 $\pm$ 0.8 kJ mol^{-1} K^{-1} for ΔC_{pf}.

DISCUSSION

Equilibrium Unfolding of Apocytochrome b_5. The equilibrium unfolding curve based on measurements of Trp fluorescence demonstrates clearly that apocytochrome b_5 denatures in a cooperative transition that can be effectively modeled on the basis of a two-state approximation. Unlike a much earlier study, the denaturation curve of apocytochrome b_5 is defined by regions in which the folded and unfolded forms predominate with a transition midpoint around ~1.6 M GuHCl (*27*). This transition midpoint is lower than that observed with the holoprotein [ref *28* and unpublished observations of S. Manyusa and D. Whitford, 1998 ($C_m \sim 3.0$ M, $\Delta G_{uw} = 23.5$ kJ mol^{-1})] and points to decreased conformational stability in the presence of this denaturant. The conformational stability at 10 °C has been estimated from the equilibrium unfolding curves to be 11.6

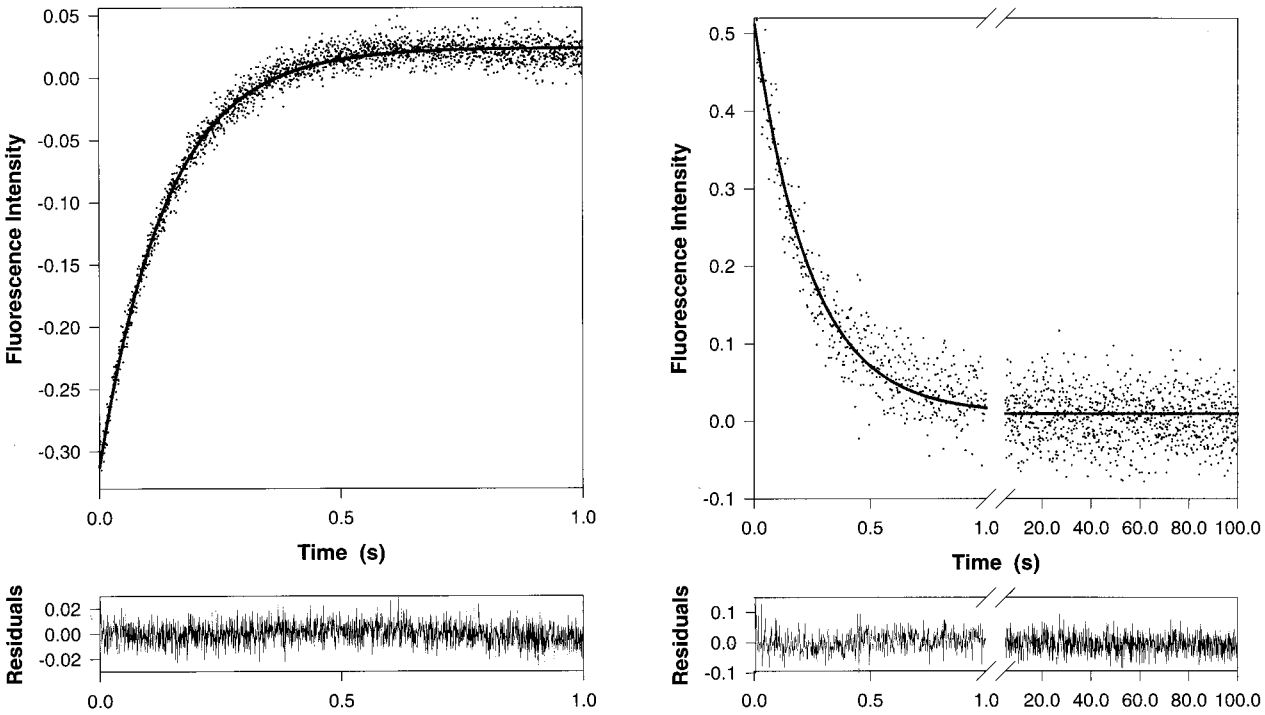

FIGURE 3: Kinetics of apoprotein unfolding and refolding determined using the change in fluorescence above 320 nm. (Left) Apocytochrome b_5 (1 μM) was rapidly mixed with 4 M GdmCl and the fluorescence measured over a time range of 1 s. The data shown together with the residuals represent the fit of the data to a single-exponential process. The residuals reveal no consistent deviation from a single-exponential process, and the unfolding reaction, in the above trace, is essentially complete after 250 ms. (Right) Refolding was carried out by rapidly mixing the unfolded protein with 30 mM MOPS (pH 7.0). The refolding reaction involved a 6-fold dilution of the unfolded protein which yielded a final denaturant concentration of 0.67 M. The trace measures refolding over 100 s to aid identification of slow refolding events such as cis−trans proline isomerization. The solid line emphasizes the monophasic process, and this is supported by the lower residuals plot.

kJ mol^{-1}. The data suggest that the heme group contributes approximately 50% (11.6/23.5 in this study) of the total conformational stability of the holoprotein via noncovalent interactions with the polypeptide chain, a value comparable to that estimated for various states of myoglobin (*29*).

Kinetic Studies of Folding and Unfolding in Apocytochrome b_5. The kinetic data obtained here for apocytochrome b_5 suggest a soluble domain in which unfolding and refolding occur without the formation of intermediates on the millisecond to second time scale. The refolding of apocytochrome b_5 was adequately fitted to a single-exponential process, and there was no evidence for the multiphasic kinetics (70, 2, and 0.06 s^{-1}) seen previously using urea as a denaturant (*15*). In general, we have found that urea and GuHCl give qualitatively similar results for both folding and unfolding pathways, and it is possible that the slower phases seen previously may result from protein aggregation, as noted in other systems (*30*). In the absence of denaturant, a maximal rate of refolding of ~20 s^{-1} was observed at 10 °C.

A two-state model for the unfolding of apocytochrome b_5 is emphasized by the observation that the equilibrium constant (K_k), estimated from the ratio of the folding and unfolding rate constants (k_{fw}/k_{uw} = 10.4 kJ mol^{-1}), agrees closely with the value of 11.6 kJ mol^{-1} obtained from equilibrium studies. The relationship $m_{eq} = m_{ku} + m_{kf}$ is satisfied with a value for $m_{ku} + m_{kf}$ of 8009 J mol^{-1} M^{-1} comparing favorably with the equilibrium value of 7874 J mol^{-1} M^{-1}. The two-state approximation is also supported by the substitution of m_{kf} by $m_{eq} - m_{ku}$ in the chevron plot of Figure 4 which yields an equally good fit of the experimental data. In many respects, apocytochrome b_5 behaves in a manner similar to that reported for CI2 and other small soluble domains (*31*). Intermediates are not detected in either folding or unfolding, and the kinetics and equilibrium folding reactions can be ascribed to a simple two-state model. These results, together with monophasic rates and an exponential dependence on denaturant concentration, provide strong evidence that apocytochrome b_5 behaves thermodynamically and kinetically as a two-state folding system.

Thermodynamic Parameters Associated with the Transition State for Folding. The activation parameters estimated via the temperature dependence of unfolding and refolding provide insight into the structure of the transition state. From Table 2, the enthalpy changes for unfolding are positive, suggesting weaker interactions exist in the transition state than in the folded form of the apoprotein. The value for $\Delta H_u^{\ddagger}$ of 120 kJ mol^{-1} reflects the loss of interactions (van der Waals interactions and hydrogen bonds) in the transition state when compared with the native state of the apoprotein. However, the hydration effect (*32*) can contribute to a loss of enthalpy from additional interactions between hydrophobic surfaces exposed during unfolding as well as ordering of solvent molecules. This effect appears to be secondary to the disruption of noncovalent interactions for the unfolding of apocytochrome b_5. In contrast, the gain in enthalpy for refolding is smaller ($\Delta H_f^{\ddagger}$ = 42 kJ mol^{-1}), and this may reflect a greater contribution of the hydration effect in a highly solvent-exposed denatured state. The entropy of the respective transition states reflects two counteracting ef-

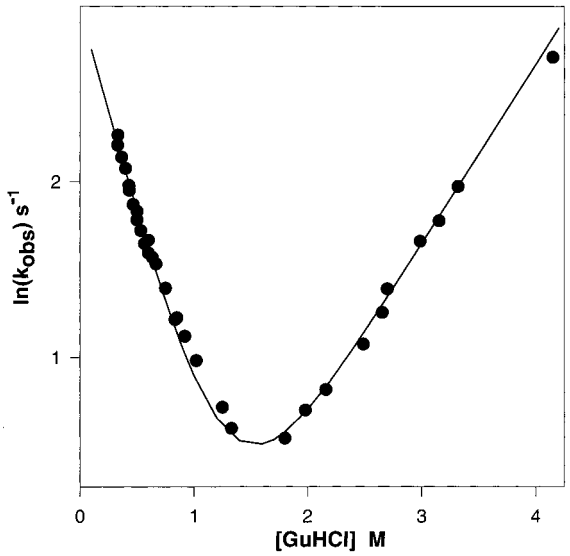

FIGURE 4: Semilogarithmic plot of kinetics of folding and unfolding of apocytochrome b_5 as a function of denaturant concentration. The chevron plot exhibits a midpoint around 1.6 M in close agreement with that estimated from equilibrium fluorescence studies. The unfolding and refolding regions of the chevron plot exhibit a linear dependency on GuHCl concentration. The line of best fit was calculated assuming the following relationship: $\ln k_{obs} = \ln(k_u + k_f)$, where $k_u = k_{uw} \exp(m_u[\text{GuHCl}])$ and $k_f = k_{fw} \exp(m_f[\text{GuHCl}])$, k_{uw} and k_{fw} are the unfolding and refolding rates in the absence of denaturant and m_u and m_f are the dependence of these rates on GuHCl concentration, respectively. Initial estimates for m_u and m_f and k_{uw} and k_{fw} were obtained by regression of a linear portion of each limb of the chevron plot and then used to fit directly to the above relationships. The data derived from this plot are summarized in Table 1.

fects: the increased conformational freedom of the protein upon unfolding versus the ordering of water molecules around nonpolar side chains. As a result, it remains difficult to assign specific molecular details to the observed changes in entropy, and it should also be kept in mind that the relevance of transition state theory and particularly the pre-exponential term to protein folding has been questioned (*33*, *34*).

In apocytochrome b_5, the changes in activation heat capacity together with the ratio of the kinetic/equilibrium *m* values assist in defining the transition state. The transition state lies close to the initial state of the apoprotein since the ratio m_{ku}/m_{eq} of ~0.3 suggests solvent accessibility analogous to that of the folded state. A value of 0.3 implies the preservation of a considerable number of noncovalent interactions in the transition state complex and is further supported by the negligible change in heat capacity ($\Delta C_{pu} \sim 0$) observed in the temperature dependence of the unfolding reaction (Figure 5A). The hydration of hydrophobic groups exposed during unfolding has been estimated to be the major contributing factor to the total heat capacity change (*35*). Here, ΔC_{pu} corresponds to the heat capacity change between native and transition states ($\Delta C_{p,\ddagger-N}$) of the protein, and its small or negligible value supports a model for the transition state in which a compact structure exists lacking significant hydration or solvent accessibility. Conversely, the refolding reaction exhibits a significant change in heat capacity between the unfolded state and the transition state estimated to be -3.6 kJ mol^{-1} K^{-1}. Using differential scanning calorimetry, the specific heat capacity of apocytochrome b_5 has been estimated to be 4.2 kJ mol^{-1} K^{-1} (*9*), and with this value, we can subsequently calculate ΔC_{pu} to be 0.6 kJ mol^{-1} K^{-1}. It is unlikely given the small magnitude of ΔC_{pu} and the experimental errors involved in these measurements that this can be detected via the Eyring analysis of the unfolding data.

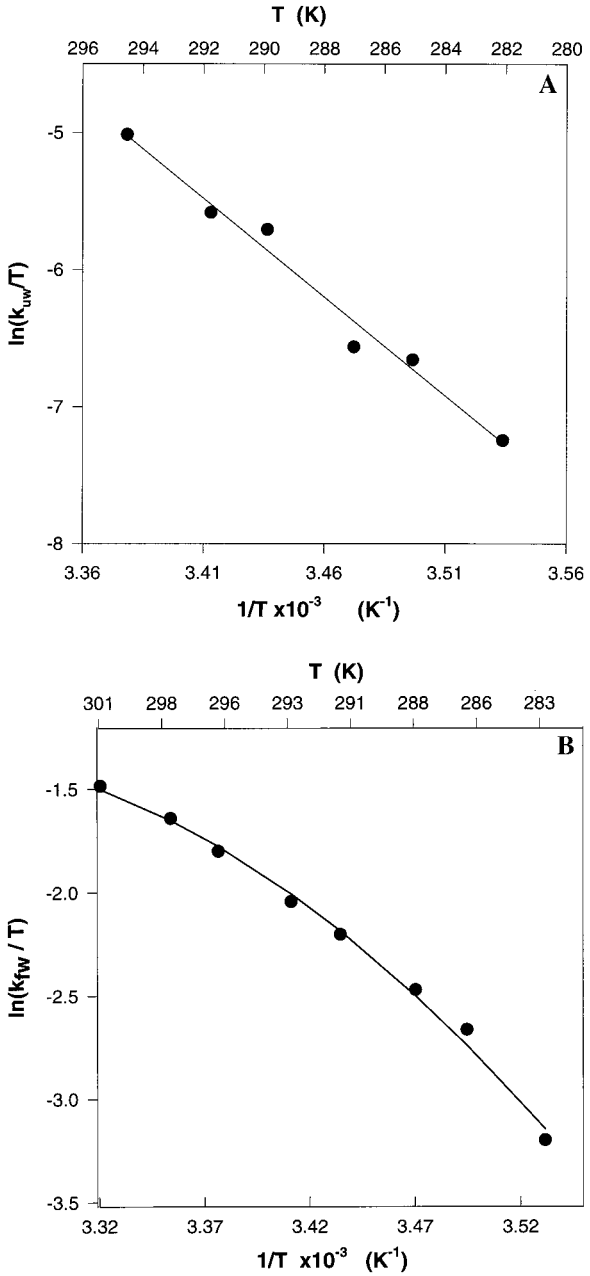

FIGURE 5: Temperature dependence associated with the refolding and unfolding reactions of apocytochrome b_5. (A) The unfolding of apocytochrome b_5. (B) The refolding of apocytochrome b_5. For each Eyring plot, the data point reflects the rate of refolding or unfolding in the absence of denaturant. This was obtained by extrapolating rates observed at different denaturant concentrations to zero GuHCl concentration at temperatures between 7 and 25 °C. Solution conditions were as described in Experimental Procedures, and the protein concentration was 1 μM. The data derived from these plots are listed in Table 2.

For apocytochrome b_5, the denaturant *m* values and the heat capacity changes point to a transition state that retains between 71 ($m_{\ddagger-U}/m_{U-N} = \theta_m$) and 86% ($\Delta C_{p,\ddagger-U}/\Delta C_{p,U-N} = \theta_{Cp}$) of the structure of the initial folded form. It has been noted that that a good correlation exists for many proteins

Table 1: Unfolding and Refolding Data for the Apo Form of Ala1−Ser104 Bovine Microsomal Cytochrome b_5[a]

method	ΔG_u (kJ mol^{-1})	m_{eq}, m_{ku}, or m_{kf} (J mol^{-1} M^{-1})
equilibrium unfolding	11.6 ± 1.5	7874 ± 181
stopped flow folding	−7.0 ± 0.1	2420 ± 420
unfolding	3.4 ± 0.2	5589 ± 552
summation of folding and unfolding data	10.4 ± 0.2	8009 ± 486

[a] All data were obtained at 10 °C in 30 mM MOPS (pH 7.0); the concentration of the apoprotein was 1 μM, and the experimental conditions were as described in Experimental Procedures.

Table 2: Activation Parameters for the Unfolding and Refolding Reactions in Apocytochrome b_5[a]

	refolding	unfolding	unfolding − refolding (equilibrium values)
ΔH(298 K) (kJ mol^{-1})	42.4 ± 5.5	119.9 ± 8.45	77.5
ΔS(298 K) (J mol^{-1} K^{-1})	−69.2 ± 18.6	165.8 ± 29.0	235.0
ΔG(298 K) (kJ mol^{-1})	63.0	70.5	7.5[b]
ΔC_p (kJ mol^{-1} K^{-1})	−3.6 ± 0.8	0.6	4.2[c]

[a] The data shown above were calculated from the Eyring plots of panels A and B of Figure 5 for the unfolding and refolding of apocytochrome b_5. The activation parameters are those obtained at zero denaturant concentration, in 30 mM MOPS (pH 7.0), and at 25 °C. In view of the detectable curvature in the refolding curve, the data were fitted to eq 6. [b] The value of 7.5 kJ mol^{-1} refers to the difference between the unfolding and refolding values obtained here at 25 °C. This value is in close agreement to that reported by Pfeil (*9*). At 10 °C, the value of ΔG has been determined in this study to be 11.6 kJ mol^{-1}. [c] The value for ΔC_{pu} was calculated using a value for ΔC_p of 4.2 kJ mol^{-1} K^{-1}, estimated by differential scanning calorimetry (*9*) and the relationship $\Delta C_p = \Delta C_{pu} - \Delta C_{pf}$.

between equilibrium measurements of the change in heat capacity upon unfolding (ΔC_{pu}) and the denaturant dependencies of protein stability (m_{eq}) (*36*). Both parameters appear to reflect the change in solvent accessible area upon folding, and by analogy, it is expected that the kinetic/equilibrium ratios derived from heat capacity ($\theta_{Cp} = 0.86$) and m value measurements ($\theta_m = 0.71$) also correlate. With due consideration of the experimental errors involved in these measurements, the respective values of θ_{Cp} and θ_m are sufficiently similar for us to believe they are defining the same transition state. For a small representative class of proteins, it was noticed that θ_{Cp} was often less than θ_m (*37*), and this was attributed to differential changes in solvent viscosity affecting the pre-exponential term in the Arrhenius equation arising as a result of increases in denaturant concentration or temperature. As a result, θ_m would overestimate transition state compactness while θ_{Cp} would tend to underestimate this parameter. Although we have the opposite situation here, it may be significant that the temperature range used in this study is more restricted than in many other systems. Combining both parameters leads to an average value for transition state compactness in which 79% of the residues buried in folding are equally inaccessible in the transition state.

Protein Folding Pathways in Apocytochrome b_5. In many proteins, refolding is accompanied by the presence of one or more minor phases arising from isomerization of prolyl−peptide bonds. The absence of minor phases in the refolding of apocytochrome b_5 suggests that these reactions are not involved in the formation of the Trp-centered hydrophobic core. In the unfolded state, the ratio of cis/trans prolyl peptide bonds is expected to be approximately 0.2. In the Ala1−Ser104 variant of apocytochrome b_5, three Pro residues exist at positions 44, 85, and 96. The identical folding properties exhibited by the shorter Ala1−Lys90 variant of cytochrome b_5 eliminates any involvement of Pro96. If one or both of the peptide bonds preceding residues 44 and 85 occur in the cis conformation, then kinetically heterogeneous folding rates would be observed. This clearly does not occur in this study where folding and unfolding have been performed over a time scale from 100 ms to 100 s, and at least two direct explanations can be invoked. The formation of the apoprotein is based around the measurement of Trp26 fluorescence and in particular the quenching mediated by His19 and solvent exclusion that accompanies protein folding. The Trp residue is located within a series of β-strands that form in the center of the molecule. Here, besides the coplanar interaction with His19, the Trp residue is close to the side chain of Ile80, and is surrounded by hydrophobic side chains at residues 27−29 as well as neighboring β-strands. This region of the protein has been described as a tube filled with hydrophobic residues exposed to solvent at either end (*4*). Both Pro residues are located away from this locus for protein folding with Pro44 forming part of the turn between helices II and III (*4*, *5*), while Pro85 is located at a turn between strand 2 and helix 6. NMR studies of apocytochrome b_5 suggest that the helices surrounding the heme binding pocket, in which Pro44 is located, are disordered, and it is most probable that any folding events in this region of the molecule occur after formation of the Trp core. For Pro85, there is some evidence to suggest that the structure of this region of the apoprotein is preserved after heme removal (*6*, *14*). It is also interesting to note that Pro44 and Pro85 are immediately following histidine residues and the motif His-Pro may not adopt the cis conformation as readily as other X-Pro residues.

An interaction between Trp26 and His19 represents an early event in the folding pathway of apocytochrome b_5. The invariance of Trp26 in all cytochrome b_5 sequences suggests the side chain may represent a locus about which protein folding occurs, and such residues have been higlighted as important in nucleation type models of protein folding (*38*). The hydrophobic side chains in this region of the protein could therefore drive the formation of the folded state via specific interactions and the exclusion of solvent, and this is supported by the comparatively large heat capacity change for refolding ($\Delta C_{pf} = -3.6$ kJ mol^{-1} K^{-1}). From the data that are presented, it is unclear whether the four helices surrounding the heme exhibit local folding within the time scale of the formation of ordered structure around Trp26. This may well require detailed analysis using additional techniques such as stopped flow CD studies or amide exchange NMR studies.

Increasingly, many small soluble proteins containing less than 100 amino acid residues have been shown to fold by a two-state mechanism, and all of these proteins are distinguished by containing only one domain in the folded state (*37*). Apocytochrome b_5 containing 104 residues is slightly larger than most of these proteins but in all other respects behaves as a typical two-state folding system. From these

observations, one may deduce that apocytochrome b_5 contains a single domain localized around Trp26.

We have shown via kinetic and equilibrium data that the unfolding and refolding of apocytochrome b_5 follow a simple two-state mechanism in which the transition state for unfolding resembles the native-like structure. The transition state is compact with most (79%) hydrophobic residues buried and with nearly all noncovalent interactions preserved. The formation of a hydrophobic core around Trp26 appears to be a key step in the folding pathway driven by the potentially large number of hydrophobic interactions in this region of the protein. This study will permit future analysis of the effect of site-directed mutagenesis of key residues of apocytochrome b_5 on the folding pathway and will importantly also allow a comparison with the potentially more complicated pathway that exists in the holoprotein.

ACKNOWLEDGMENT

Dr. Katalin Torok (School of Biological Sciences, Queen Mary & Westfield College) is thanked for providing frequent access to an SLM-Aminco 8100 fluorimeter.

REFERENCES

1. Fersht, A. R. (1993) *FEBS Lett. 325*, 5−16.
2. Kim, P. S., and Baldwin, R. L. (1990) *Annu. Rev. Biochem. 59*, 631−660.
3. Zaidi, F. N., Nath, U., and Udgaonkar, J. B. (1997) *Nat. Struct. Biol. 4*, 1016−1024.
4. Mathews, F. S., Czerwinski, E. W., and Argos, P. (1979) in *The Porphyrins* (Dolphin, D., Ed.) Vol. 7, pp 107−147, Academic Press, New York.
5. Muskett, F. W., Kelly, G. P., and Whitford, D. (1996) *J. Mol. Biol. 258*, 172−189.
6. Arnesano, F., Banci, L., Bertini, I., and Felli, I. C. (1998) *Biochemistry 37*, 173−184.
7. Newbold, R. J., Hewson, R., and Whitford, D. (1992) *FEBS Lett. 314*, 419−424.
8. Hewson, R., Newbold, R. J., and Whitford, D. (1993) *Protein Eng. 6*, 953−964.
9. Pfeil, W. (1993) *Protein Sci. 2*, 1497−1501.
10. Huntley, T. E., and Strittmatter, P. (1972) *J. Biol. Chem. 247*, 4641−4647.
11. Provencher, S. W., and Glockner, J. (1981) *Anal. Biochem. 155*, 155−167.
12. Johnson, W. C., Jr. (1990) *Proteins: Struct., Funct., Genet. 7*, 205−214.
13. Falzone, C. J., Mayer, M. R., Whiteman, E. L., Moore, C. D., and Lecomte, J. T. G. (1996) *Biochemistry 35*, 6519−6526.
14. Moore, C. D., and Lecomte, J. T. J. (1990) *Biochemistry 29*, 1984−1989.
15. Moore, C. D., and Lecomte, J. T. J. (1993) *Biochemistry 32*, 199−207.
16. Shawver, L. K., Seidel, S. L., Kreiter, P. A., and Shires, T. K. (1984) *Biochem. J. 217*, 623−632.
17. Jones, M. S., and Jones, O. T. G. (1969) *Biochem. J. 113*, 507−514.
18. Barrick, D., and Baldwin, R. L. (1993) *Protein Sci. 2*, 869−876.
19. Goto, Y., and Fink, A. L. (1994) *Methods Enzymol. 232*, 3−15.
20. Jennings, P. A., and Wright, P. E. (1993) *Science 262*, 892−896.
21. Pace, C. N. (1986) *Methods Enzymol. 131*, 266−279.
22. Strittmatter, P. (1960) *J. Biol. Chem. 235*, 2492−2497.
23. Teale, F. W. J. (1959) *Biochim. Biophys. Acta 35*, 543.
24. Laidler, K. J. (1950) *Chemical Kinetics*, McGraw-Hill, New York.
25. Tan, Y.-J., Oliveberg, M., and Fersht, A. R. (1996) *J. Mol. Biol. 264*, 377−389.
26. Gopalan, V., Golbik, R., Schreiber, G., Fersht, A. R., and Altman, S. (1997) *J. Mol. Biol. 267*, 765−769.
27. Tajima, S., Enomoto, K.-I., and Sato, R. (1976) *Arch. Biochem. Biophys. 172*, 90−97.
28. Vergeres, G., Chen, D. Y., Wu, F.-F., and Waskell, L. (1993) *Arch. Biochem. Biophys. 305*, 231−241.
29. Hargrove, M. S., Wilkinson, A. J., and Olson, J. S. (1996) *Biochemistry 35*, 11310−11318.
30. Utiyama, H., and Baldwin, R. L. (1986) *Methods Enzymol. 131*, 51−70.
31. Jackson, S. E., and Fersht, A. R. (1991) *Biochemistry 30*, 10428−10435.
32. Kauzmann, W. (1959) *Adv. Protein Chem. 14*, 1−63.
33. Chen, X., and Matthews, C. R. (1994) *Biochemistry 33*, 6356−6362.
34. Scalley, M. L., and Baker, D. (1997) *Proc. Natl. Acad. Sci. U.S.A. 94*, 10636−10640.
35. Privalov, P., and Makhatadze, G. I. (1992) *J. Mol. Biol. 224*, 715−723.
36. Myers, J. K., Pace, C. N., and Scholtz, J. M. (1995) *Protein Sci. 4*, 2138−2148.
37. Plaxco, K. W., Simons, K. T., and Baker, D. (1998) *J. Mol. Biol. 277*, 985−994.
38. Shakhnovich, E., Abkevich, V., and Ptitsyn, O. (1996) *Nature 379*, 96−98.

BI990550D